

Detecting 2D NMR Signals Using Mask RCNN

Hadeel Saad Alghamdi¹, Alexei Lisitsa¹, Igor Barsukov² and Rudi Grosman²

¹Computer Science, University of Liverpool, U.K.

²Biochemistry & Systems Biology, University of Liverpool, U.K.

Keywords: NMR Spectre Analysis, Peak Detection, Mask R-CNN.

Abstract: Picking peaks in two-dimensional Nuclear Magnetic Resonance (NMR) spectra has been a critical research problem and a very time-consuming important step in further analyses of NMR biological molecular systems. Here, we implemented machine learning approach for peak detection and segmentation using machine learning framework Mask R-CNN. The model was trained on a large number of synthetic spectra of known configurations, and we show that our model demonstrates promising results up to 0.93 accuracy. We implemented uniform scaling on the data matrix during training to further improve detection to achieve 10.17% FPs and 1.7% FNs rate. We show the utility of Mask R-CNN on NMR spectra where the data range plays an important role in peak detection.

1 INTRODUCTION

Nuclear Magnetic Resonance (NMR) spectroscopy is one of most powerful technique for the confirmation of structural identity and for structure elucidation of unknown compounds (Elyashberg, 2015). NMR spectroscopy is a widely popular approach (K., 1986) as it provides information on the molecular structure of complex chemical compounds and mixtures. It finds its applications in various areas including medical diagnosis, drug discovery by monitoring inter molecular interactions (Pellecchia et al., 2008), and identifying components by screening complex mixtures in various environmental science studies. One of the critical steps in NMR structure determination is peak picking (Pellecchia et al., 2008). A typical 2D spectrum (see Fig. 1) can contain hundreds to thousands of peaks, and the identification and quantitative characterization of those peaks has a significant impact on all downstream analyses and further data interpretation. Each peak is distinguished by its centre position (frequency coordinates corresponding to, so called chemical shifts), peak shape along each dimension and peak amplitude (Hesse et al., 2007). The following steps are invariably entailed in the analysis of an NMR spectrum: (i) identification of the entire set of peaks, known as peak picking; (ii) assignment of each peak to the atoms it belongs to; and (iii) quantification of each peak by determining the peak amplitude or volume (Li et al., 2021). These steps have been only

be partially automated despite years of progress. The biggest difficulty in automation peak picking comes from picking peaks in small molecular and distinguishing them from artifacts making this task tiring, time-consuming and complicated without expert human assistance.

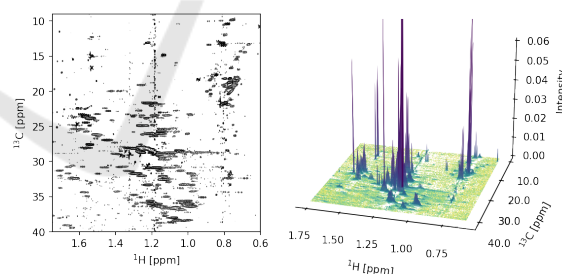


Figure 1: High resolution 2D NMR spectrum section of a complex mixture. Typically NMR data range is between 0-12 ppm on ¹H and 0-200 ppm on ¹³C. Left panel shows the typical contour visualisation of the data used during analyses. Right panel shows the same data in a 3D visualisation.

Numerous approaches have been proposed to solve this problem. These include picking signals based on their intensities, volumes, or local signal-to-noise ratio and are frequently combined with methods that improve spectrum quality, such as wavelet transform (Liu et al., 2012), Bayesian methods (Cheng et al., 2014) and spectra-decomposition-based methods (Tikole et al., 2014). Semi manual peak picking

usually provides more precise results with the assistance of interactively picking features of common NMR software such as POKY(Goddard and Kneller, 2007), NMRView (Johnson and Blevins, 1994), CCPN (SP et al., 2016) and some popular commercial packages such as TopSpin and Mnova. The applications of various machine learning techniques for NMR peak picking have been studied over the years. These include multi-layer back-propagation artificial neural networks (Corne et al., 1992), support vector machines (Klukowski.P and al, 2015), and variants of deep learning (Li et al., 2021) among others. These approaches mainly targeted peak recognition in large protein molecules. Low intensity peaks in small molecules is still a challenge up to date.

Here, we introduce a more generalized NMR spectral peak picking method, using Mask R-CNN(He et al., 2017) to automatically localize, segment and classify peaks and their Full Width Half Height area (FWHH) in both large and small molecules. We report our preliminary results obtained by using synthetic datasets of artificial spectra with the small number of peaks for training Mask-R-CNN models. We present tuning of default Mask-R-CNN configurations and study the effects of scaling of data. Overall performance appears to be promising (up to 93% accuracy), but it requires further systematic evaluation on more realistic spectra with the larger amounts of peaks.

2 PEAKS IN NMR SPECTRA

Due to exponential decay of the NMR signals the peaks have a theoretical Lorentzian line shape. However, the use of window functions in the processing of 2D NMR data leads to the shape changes that can be approximated by a mixture of Gaussian and Lorentzian functions (Davis et al., 2020). Therefore, we used both of the functions $G(x,y)$ and $L(x,y)$ to generate the data for the training:

$$G(x,y) = \frac{1}{\sigma\sqrt{2\pi}} \exp \left[-\frac{(x-x_0)^2}{2\sigma^2} + \frac{(y-y_0)^2}{2\sigma^2} \right]$$

$$L(x,y) = \frac{1}{\pi\gamma \left[1 + \left(\frac{x-x_0}{\gamma} + \frac{y-y_0}{\gamma} \right)^2 \right]}$$

Fig. 2 demonstrates peaks modelled by Gaussian and Lorentzian functions. The height of the peaks is represented by the color.

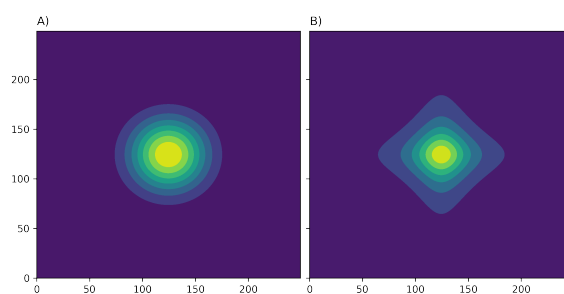


Figure 2: Filled contours of peaks calculated with A) Gaussian functions on both dimensions and B) Lorentzian function on both dimensions.

3 METHOD

3.1 Mask R-CNN Framework

Mask R-CNN is a deep neural network aimed to solve instance segmentation problem in machine learning or computer vision (He et al., 2017). Mask R-CNN model is commonly used for object detection and segmentation. It has usefully been trained to detect and segment objects in various areas including medicine, (Chiao et al., 2019). planetary science (Davis et al., 2020) and engineering (Zhao et al., 2018). The Input in most of those cases is originally an image in RGB format with relatively large and well outlined objects. In contrast, the NMR peaks are not confined to a well-defined region of the spectrum. Their intensities gradually decrease, but in the absence of noise, are theoretically present in any part of the spectrum. The noise in the experimental spectra makes the peak contribution undetectable once it falls below the noise level, however for each peak this boundary depends on the peak amplitude, line-width and shape. This presents a major challenge in assigning a mask to the peak. If, similar to objects in photographs, the mask is considered as the area outside of each no contribution from the peak can be detected, no mask can be assigned in the absence of noise, while the different degree of noise would change the mask of the same peak object, making the mask dependent on the conditions rather than on the peak properties. Additionally, peaks in the NMR spectra have wide range of amplitudes, and the overall spectra are arbitrary scaled during the measuring and data processing, while in the images there is an objective image scaling, and much more limited range of intensities. To address these challenges in the practical NMR spectroscopy, the cross-section at half-height is used to characterise the peak, which is only dependent on the peak parameters, but not on the amplitude or noise level. This area is straightforward to calculate theoretically, mak-

ing it objective and suitable for generation of training data. And prediction of this mask would be much more informative in the real data analysis as it will directly reflect the peak parameters. However, as illustrated in Fig.4, the half-height mask is much smaller than the total area of the detectable peak intensities. It is unclear whether Mask R-CNN developed for the recognition of well-defined shapes is suitable for the analysis of "diffused" objects, such as NMR peaks, that do not have a well-defined invariable mask that covers the whole object. In this study we investigate a general applicability of Mask R-CNN to the recognition of peaks in the NMR spectra.

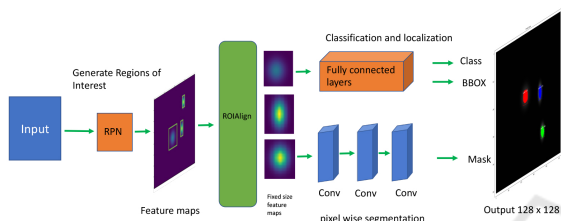


Figure 3: Mask R-CNN structure.

Fig. 3 outlines the architecture of Mask R-CNN. It consists of a pre-trained CNN network on image classification tasks to generate feature maps of the input. Region Proposal Network (RPN) slides a window over the feature maps to generate anchors for each image. The anchors are used then by RPN to generate Regions of Interest (RoI) which bounding box that may or may not contain a peak. Mask R-CNN handles RoIs without digitizing thus yielding feature maps of fixed sized. The feature maps are fed into fully connected layers to make classification, where boundary box prediction is refined using the regression. The warped features are also fed into Mask branch classifier in parallel in the existing branches for classification and localization. The mask branch is a small fully connected network (FCN) applied to each RoI predicting a pixel wise segmentation mask of the object (He et al., 2017).

3.2 Mask Calculation

Training data for Mask R-CNN contains two forms of input, the target objects and corresponding masks. The masks in our dataset is calculated to cover the area at *full width half height* (FWHH) values around each peak.

Fig. 4 demonstrates the mask area which doesn't cover the whole object (peak) as it is the case in most object detection projects.

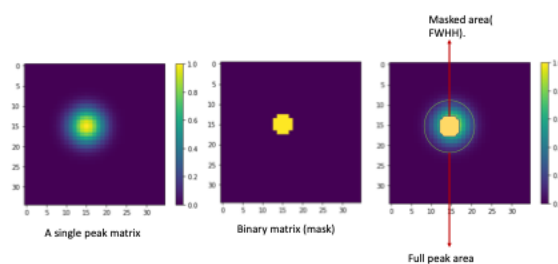


Figure 4: Mask covers only FWHH area.

3.3 Dataset

The dataset is synthetically generated using NMRglue (Helmus and Jaroniec, 2013), a python library package for NMR analysis. Each generated spectrum contains a number of peaks with the following properties:

1. Spectra are generated as matrices of 64-bit floats.
2. Each matrix has a shape of 128x128 (minimum size for Mask R-CNN (He et al., 2017)).
3. Each matrix contains k peaks randomly located, where $k = [1..4]$ with uniform distribution.
4. The peaks are either Gaussian at both axis or Gaussian at one axis and Lorentzian at the other.
5. Maximum amplitude = 1.
6. Masks are calculated to cover the area of full width half height (FWHH) values around each peak (local maximum) (see Fig. 5 for an illustration).



Figure 5: Three peaks and their masks.

7. No noise present during the training.
8. No overlapping masks present.

3.4 Pre-Processing

Mask R-CNN have been primarily applied to the recognition of natural images, which feature perspective (distance-size dependence, e.g. objects placed further appear smaller), fixed aspect ratio and are regular grids of discrete-value pixels (0–255 in RGB space). Mask R-CNN applies some standard pre-processing procedures (He et al., 2017) to the input data such as:

1. Non-square data is resized to square shape by Re-size and pad with zeros to get a square shape.
2. Inputs must have three channels.

3. Input data is converted to 32-bit floats followed by subtraction of mean value. Post training, mean value is added back and data is converted to 8-bit integers.

4. Batch Normalization Layers are frozen by default.

The model was trained in two implementation scenarios where the first one as standard as possible and the second one with sensible changes better suited to the nature of our data.

3.5 Evaluation Criteria

For evaluation of the results of training we use mAP measure and the rates of False Positive (FP) and False Negative (FN) detections. mAP is a evaluation metric used in Mask R-CNN for object localisation and classification(Everingham et al., 2010). The definitions of FP and FN should take into account not only predicted classes but also the locations of predicted bounding boxes. Hence we define TP, FP, FN as follows. In Mask-R-CNN the predicted detection $\{(b_j, c_j, p_j)\}$ indexed by object j consists of:

- Bounding Box (BB) b_j ,
- predicted class ('peak' or 'no peak' in our case) c_j ,
- confidence score p_j .

A predicted detection (b, c, p) is regarded as a True Positive (TP) if:

- The predicted category c equals the ground truth label c_g .
- The overlap ratio IOU (Intersection Over Union)(Everingham et al., 2010).

$$\text{IOU}(b, b^g) = \frac{\text{area}(b \cap b^g)}{\text{area}(b \cup b^g)}$$

between the predicted bounding box b and the ground truth bounding box b^g is not smaller than a predefined threshold ϵ . A predicted detection (b, c, p) is regarded as a False Positive (FP) if:

- shared a ground truth with another detection (i.e both predicted detection have IOU with the same ground truth bounding box in excess of ϵ) which has higher confidence score p_j , or
- has no ground truth bounding box with IOU greater than ϵ .

A False negative (FN) is detected if:

- a ground truth peak is found without predicted bounding box with IOU greater than ϵ

The occurrences False Positives and True Positives detections are illustrated in Fig. 6.

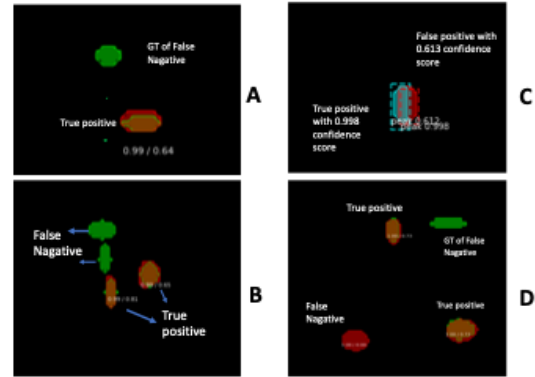


Figure 6: A, B, C and D display TP, FP and FN in different scenarios.

4 STANDARD IMPLEMENTATION

We use the implementation of Mask-R-CNN available at (He et al., 2017). The model hyper parameters are listed in Table 1.

Table 1.

Hyper parameters	Value	Definition
BACKBONE	resnet50	The backbone networks
DETECTION_MIN_CONFIDENCE	0.9	Minimum confidence threshold to accept the final detected ROI
CHANNEL_NUMBER_COUNT	3	number of channel is 3 for RGB In our case, we kept it 3 by replicating the same channel three times
IMAGE_MAX_DIM	128 x 128	Define input image resizing (none)
TRAIN_BN	Freeze	Train or freeze batch normalization layers
Number_OF_EPOCHS	20 - 90	define the number of epochs

4.1 Detection Results

Starting with 700 spectra data size, and the Testing method used here is the traditional 20/80 split. The model scored a mAP of 0.660 with 2.15 % of FPs and FNs 19 % of FNs. More detailed analysis was conducted of the detected peaks by extracting their details such as height, width and data mean of a whole spectra, they fall into three categories:

- Correctly Detected Peaks: peaks with maximum value ≥ 3.4 are correctly detected and classified.
- Valid peaks with overlapped false peaks: valid peaks with corresponding Ground Truth GT, those peaks have also false overlapped peaks.

- **Not Detected Peaks:** missed peaks where they have GT, but the model failed to detect them. The majority of the those peaks have maximum value ≤ 3.4 .

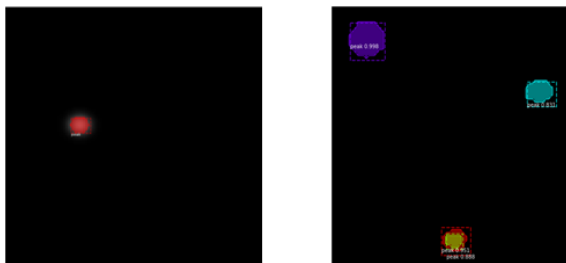


Figure 7: Detected peaks.

To better understand the detection results and improve the accuracy we have applied *magnitude scaling* for the data. Here we have relied also on the fact that all essential information in NMR spectra is magnitude-invariant, that is scaling up or down by a constant factor does not change the information content of NMR spectra, but it may well affect the performance of machine learning algorithms on the data. In practice one can also should take into account the scaling limitations caused by a particular implementation (e.g by the range of datatype values available).

In Table 2 we represent the detection results for various scaling factors applied to testing phase only. Then the range mean is calculated. The range is defined here as the difference between the maximum and minimum values for each spectra then taking the mean of those values for whole testing dataset.

Table 2.

Scaling factor	Range mean	mAP	FPs %	FNs %
No scaling	0.697	0.660	2.150	19.120
5	3.785	0.751	2.370	9.762
10	7.350	0.769	1.280	7.710
15	11.010	0.771	1.080	7.310
50	34.900	0.817	2.720	7.900
100	69.000	0.815	3.000	8.700
150	97.560	0.841	0.540	7.560
200	145.230	0.813	1.560	6.510
255	177.450	0.781	2.460	8.760

As seen from the table the model started performing better when the data mean between 34.90 and 177.23. Since the scaling was only applied during testing and to form a complete conclusion, Table 3 shows the outcomes of training the model with scaling during: both training and testing, training only and testing only. The scaling factor is determined by selecting the best preformed model from Table 2 which is 150.

Table 3.

Scaling applied	mAP	FPs %	FNs %
No scaling	0.660	2.150	19.120
Train & Test	0.898	6.480	6.940
Train only	0.579	8.5	13.9
Test only	0.781	2.460	8.760

Scaling during testing only or training and testing combined show similar results.

4.2 Larger Dataset Size

To eliminate the possibility of inefficient number of training samples, we generated bigger dataset (5k spectra). The dataset description and hyper parameters are the same as 700 spectra data size. The model scored a mAP of 0.616 with 12.15% of FPs and FNs 31% of FNs. Table 4 presents the scaling results during the testing stage, and it displays decline in FP and FN percentage when the data ranges from 2.52 to 7.104 and an increase in mAP score

Table 4.

Description	Range mean	mAP	FPs %	FNs %
No scaling	0.5002	0.616	12.19	31.55
5	2.5200	0.630	12.01	9.81
10	4.7690	0.684	10.61	8.90
15	7.1040	0.686	9.10	11.55
50	25.4770	0.557	8.36	21.25
100	48.8730	0.549	8.09	17.78
150	73.1000	0.489	12.32	20.24
200	100.7300	0.464	10.82	18.67
255	122.4400	0.492	11.59	16.60

Similar to the 700 dataset, scaling was also applied during the three stages. However, scaling during training and testing combined outperformed the other scenarios as shown in Table 5.

Table 5.

Scaling applied	mAP	FPs %	FNs %
No scaling	0.616	12.19	31.55
Train & Test	0.784	7.27	2.59
Train only	0.781	3.19	16.66
Test only	0.492	11.59	16.60

Finally, The two best preformed models are selected by scaling to the optimal data range and trained with the optimal number of epochs see Table 6.

- Scaling of the range mean between 83.23 and 122.7.

- Scaling in both the training and testing stages.

Table 6.

Data size	mAP	FPS %	FNs %
700	0.788	0.400	1.200
5k	0.971	1.160	2.320

5 ADJUSTED IMPLEMENTATION

As mentioned in the previous section, most undetected peaks that have maximum value ≤ 3.4 . Those peaks are relatively small and that might be a reason for low performance of Mask R-CNN standard implementation. In order to improve performance we have made several changes to the framework.

5.1 Modified Normalization

The default Mask R-CNN pre-processing in explained in Section III-D, converts floats into integers directly causing the values to be floored to 0. In order to preserve the data the pre-processing was modified. Fig.8, shows the effects of standard normalization (upper part) and modified normalization (bottom part). The bottom part of the figure shows the modified method where the subtraction of zeros (instead of mean value) and the conversion to original datatype (float64) instead to uint8 has been applied.

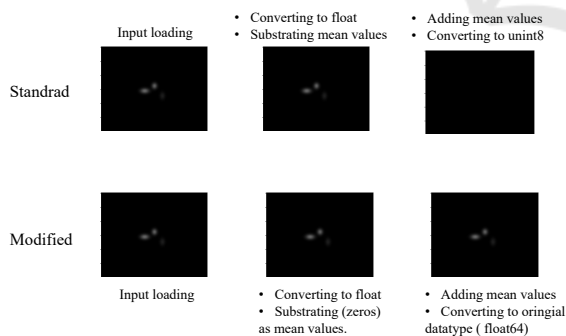


Figure 8.

5.2 Batch Normalization Layers

Mask R-CNN’s default Batch normalization (BN) layer setting are to freeze during training and used during predicting phase where the mean values provided in configuration file subtracted from the data. Here, we experimented to determine in our set-

tings whether to freeze, train or use BN layers in training mode during prediction. The detection results have improved significantly by training the BN layers, as shown in Fig. 9.

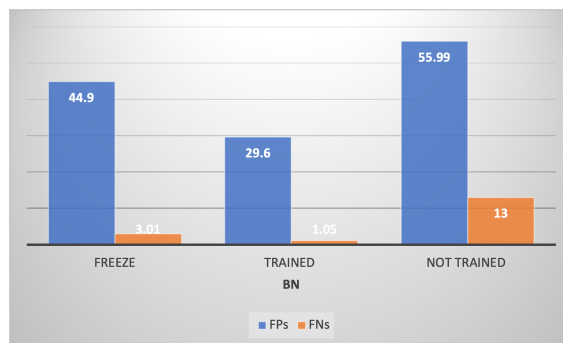


Figure 9: BN Layers tests.

5.3 Input Normalization

Mean values are used in Mask-RCNN for input normalization. Here we tested whether to use the calculated mean values or standard deviation for input normalization is better for our datatype. The model is trained with:

- 90 epochs.
- The BN layers are trained.
- The STD and Mean values are calculated across the dataset (5k).

Table 7.

Input normalization	mAP	FPS %	FNs %
calculated mean	0.91	35.50	0.46
calculated Std	0.93	10.17	1.79

The results of experiments are shown in the Table 7. They indicate the advantage of using STD for input normalization as as in this case the model demonstrates good performance with only 10.17 % FPs and only 1.7 % FN. Fig. 10 displays the final Mask R-CNN model for peaks detection and segmentation of 2D NMR spectra which gives 0.93 mAP with 10.17% FPs and only 1.79% FN.

6 DISCUSSION

In this paper, we are presenting an implementation of Mask R-CNN for 2D NMR peak picking trained with synthetic data. We have evaluated the default setting used in image segmentation for NMR data. Our findings showed us that although NMR data can be treated

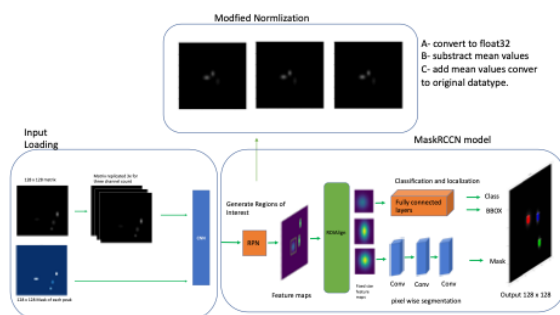


Figure 10: NMR Mask-RCNN Model.

as an image the defaults used in Mask R-CNN does not perform sufficiently. We have opted for avoiding data type conversions in order to preserve the information in the NMR data which were initially lost. Following hyper-parameter tuning, we observed poor detection on low intensity peaks. In order to increase our detection, we implemented uniform scaling on the data matrix during training. In this further improved pipeline we have achieved greater performance with 0.90 mAP, 10.17% FP and 1.7% FNs with a scaling factor of 150. The necessity of scaling is most likely due to the nature of the NMR data. Regular pictures have very clear borders between object; in the case of NMR, the objects (peaks) in the picture (spectra) has gradually disappearing borders. When the object of interest is intrinsically smaller (low intensity peak), it is particularly challenging to differentiate between the baseline, borders and the maxima. Thus, applying some prior to training can make these feature more detectable by Mask R-CNN. Our conclusion is that this framework is promising and needs further investigations. Further directions include in particular considering more realistic spectra with multiple possibly overlapping peaks and testing on both synthetic and real experimental data.

REFERENCES

- Cheng, Y., Gao, X., and Liang, F. (2014). Bayesian peak picking for nmr spectra. *Genomics, proteomics & bioinformatics*, 12(1):39–47 doi: 10.1016/j.gpb.2013.07.003. Epub 2013 Oct 31. PMID: 24184964; PMCID: PMC4411369.
- Chiao, J.-Y., Chen, K.-Y., Liao, K. Y.-K., Hsieh, P.-H., Zhang, G., and Huang, T.-C. (2019). Detection and classification the breast tumors using mask r-cnn on sonograms. *Medicine*, 98(19):e15200. doi: 10.1097/MD.00000000000015200. PMID: 31083152; PMCID: PMC6531264.
- Corne, S. A., Johnson, A. P., and Fisher, J. (1992). An artificial neural network for classifying cross peaks in two-dimensional nmr spectra. *Journal of Magnetic Resonance (1969)*, 100(2):256–266.
- Davis, C. C., Champ, J., Park, D. S., Breckheimer, I., Lyra, G. M., Xie, J., Joly, A., Tarapore, D., Ellison, A. M., and Bonnet, P. (2020). A new method for counting reproductive structures in digitized herbarium specimens using mask r-cnn. *Frontiers in Plant Science*, 11:1129 doi: 10.3389/fpls.2020.01129. PMID: 32849691; PMCID: PMC7411132.
- Elyashberg, M. (2015). Trac trends anal. *Structure–Spectrum Correlations and Computer-Assisted Structure Elucidation Joao Aires de Sousa*.
- Everingham, M., Van Gool, L., Williams, C. K., Winn, J., and Zisserman, A. (2010). The pascal visual object classes (voc) challenge. *International journal of computer vision*, 88:303–338.
- Goddard, T. and Kneller, D. (2007). Sparky 3. san francisco: University of california.
- He, K., Gkioxari, G., Dollar, P., and Girshick, R. (2017). "mask r-cnn". *Mask r-cnn. In, 2017 IEEE International Conference on Computer Vision (ICCV)*, pages 2980–2988 doi: 10.1109/ICCV.2017.322.
- Helmus, J. J. and Jaroniec, C. P. (2013). Nmr-glue: an open source python package for the analysis of multidimensional nmr data. *Journal of biomolecular NMR*, 55:355–367 http://dx.doi.org/10.1007/s10858--013--9718--x.
- Hesse, R., Streubel, P., and Szargan, R. (2007). Product or sum: Comparative tests of voigt, and product or sum of gaussian and lorentzian functions in the fitting of synthetic voigt-based x-ray photoelectron spectra. *Surface and Interface Analysis: An International Journal devoted to the development and application of techniques for the analysis of surfaces, interfaces and thin films*, 39(5):381–391.
- Johnson, B. A. and Blevins, R. A. (1994). Nmr view: A computer program for the visualization and analysis of nmr data. *Journal of biomolecular NMR*, 4(5):603–614.
- K., W. (1986). Nmr of proteins and nucleic acids', new york: John wiley and sons, [online]. https://www.europhysicsnews.org/articles/epn/pdf/1986/01/epn19861701p11.
- Klukowski, P. and al (2015). Computer vision-based automated peak picking applied to protein nmr spectra. *Bioinformatics*, pages 2981–2988.
- Li, D.-W., Hansen, A. L., Yuan, C., Bruschiweiler-Li, L., and Bruschweiler, R. (2021). Deep picker is a deep neural network for accurate deconvolution of complex two-dimensional nmr spectra. *Nature communications*, 12(1):5229. doi: 10.1038/s41467-021-25496-5. PMID: 34471142; PMCID: PMC8410766.
- Liu, Z., Abbas, A., Jing, B.-Y., and Gao, X. (2012). Wavpeak: picking nmr peaks through wavelet-based smoothing and volume-based filtering. *Bioinformatics*, 28(7):914–920.
- Pellicchia, M., Bertini, I., Cowburn, D., Dalvit, C., Giralt, E., Jahnke, W., James, T. L., Homans, S. W., Kessler, H., Luchinat, C., et al. (2008). Perspectives on nmr in drug discovery: a technique comes of age. *Nat Rev*

- Drug Discov.*, 7(9):738–745 doi: 10.1038/nrd2606. PMID: 19172689; PMCID: PMC2891904.
- SP, S., R, F., W, B., TJ, R., LG, M., and GW, V. (2016). Ccp-nmr analysisassign: a flexible platform for integrated nmr analysis. *Journal of Biomolecular NMR*.
- Tikole, S., Jaravine, V., Rogov, V., Dötsch, V., and Güntert, P. (2014). Peak picking nmr spectral data using non-negative matrix factorization. *BMC bioinformatics*, 15:46 doi: 10.1186/1471-2105-15-46. PMID: 24511909; PMCID: PMC3931316.
- Zhao, K., Kang, J., Jung, J., and Sohn, G. (2018). Building extraction from satellite images using mask r-cnn with building boundary regularization. In *IEEE/CVF Conference on Computer Vision and Pattern Recognition Workshops (CVPRW)*, pages 242–2424 doi: 10.1109/CVPRW.2018.00045.

